Density Functional Study of the Structures of Lead Sulfide Clusters $(PbS)_n$ ($n = 1-9$)

Hongxia Zeng, Zoltan A. Schelly,* Kaori Ueno-Noto, and Dennis S. Marynick*,†

Department of Chemistry and Biochemistry, University of Texas at Arlington, Arlington, Texas 76019-0065

Received: June 28, 2004

The structures of $(PbS)_n$ ($n = 1-9$) clusters are investigated with density functional theory at the B3LYP level. Various pseudopotential basis sets on lead and the 6-31+G* basis set on sulfur were employed. Full geometry optimization and extensive searches of the potential energy surface were carried out for clusters with $n = 1-6$. We find that even small PbS clusters ($n > 2$) start to take on the characteristic features of the rock salt structure of solid-state PbS (galena). The origin of some of the structural aspects of these crystals is shown to be associated with the partial covalent nature of the Pb−S bond. The magnitude of the HOMO-LUMO gap oscillates with increasing size of the clusters, in agreement with the observed behavior of the corresponding UV absorption bands of ultrasmall PbS quantum dots. Direct conformation of this oscillation was found by CIS(D) calculations, for which the absorption with the largest oscillator strength oscillates as the clusters grow from PbS to $(PbS)_9$.

Introduction

PbS (galena) quantum dots have attracted considerable attention for their potential use in optical switches, diode lasers, long-wavelength imaging, and electroluminescent devices.[1−3] Lead sulfide quantum dots have been synthesized and doped by various methods.[4−8] Compared with II−VI (CdS or CdSe) quantum dots, PbS exhibits a very strong quantum size effect (QSE) manifested in a large blue shift of its absorption band with a small decrease in cluster size.[9,10] According to the effective-mass model of Brus,[11] this can be attributed to the large radii and small effective masses of the electron and hole. This model, however, was found by Wang et al.[12] to be inaccurate for quantum dots smaller than 30 Å. They developed two new models by considering the effect of band nonparabolicity. By using a basis set of sp^3 hybrids on the lead and sulfur atoms, they explained the QSE phenomena for PbS particle sizes down to 25 Å. Several other theoretical studies of PbS quantum dots have appeared. Lippens and Lannoo[13] used a semiempirical tight-binding method to model the size dependency of the band gap of CdS, CdSe, and ZnS, and demonstrated good agreement of the results with experiment. Kane et al.[14] also used a semiempirical tight-binding method to calculate the electronic structure of spherical PbS nanocrystals. The size dependence of the band gaps was studied for clusters containing from 8 to 912 atoms. Tudury et al.[15] calculated the electronic structure of spherical PbS quantum dots by using a four-band envelope-function formalism; their results show that the band anisotropy is more pronounced for the excited states and increases with the confinement. Ab initio Hartree−Fock calculations[16,17] have also been used to investigate the band gap dependence of galena clusters.

Despite this significant body of theoretical work on PbS nanocrystals, there are no published studies on the *structures* of these very small clusters. As demonstrated by earlier work on AgBr and CdS clusters,[18−21] the structures of ultra small quantum dots bear little or no resemblance to those of the bulk. In addition, the QSE in the molecular size regime is quite different than that in the nanometer region. Both $(AgBr)_n$ and $(CdS)_n$ show an initial blue shift of their absorption bands upon cluster growth from $n = 1$ to $3-5$, followed by red shifts for larger clusters.[18,21] These blue shifts cannot be explained by an effective mass model, but are easily accounted for by density functional theory (DFT) calculations, which take into account the details of the orbital interactions and covalent effects.

In this paper, we present the first DFT study of small $(PbS)_n$ clusters ($n = 1-9$). We show that, unlike the previously studied AgBr and CdS clusters, the HOMO-LUMO gaps and binding energies oscillate with increasing cluster size, and remarkably small clusters already begin to take on the characteristic rock-salt structure of galena. In addition, we demonstrate that Pb−S interactions dominate the structural features of these clusters. This is in stark contrast to the AgBr and CdS systems, where we have previously shown that metal−metal interactions are of prime importance in determining the structures. The oscillation of the HOMO-LUMO gaps has been confirmed experimentally by the time-dependent UV spectra of growing PbS quantum dots prepared in the molecular size regime.[22]

Computational Details

All calculations were done with the Gaussian 98[23] or Gaussian 03[24] suite of programs. Gradient corrected DFT calculations with the B3LYP[25,26] functional were used for all geometry optimizations. The basis sets for lead and sulfur were SBKJC[27] and 6-31+G*, respectively. Additional basis sets, described in Table 1, were used to verify the acceptability of this basis set for both geometries and energetics. Because the minimum energy structures for each cluster were unknown, several initial guess structures were investigated. These included structures analogous to those found in our previous computational studies of AgBr and CdS, and a wide variety of polyhedral structures. Less extensive searches were performed for the largest clusters $(PbS)_n$, $n > 6$. Analytical frequency calculations were performed in all cases. Structures which had imaginary frequencies were distorted along the imaginary frequency mode until a true

† Corresponding author. E-mail: dennis@uta.edu.

10.1021/jp040457l CCC: $30.25
Published on Web 02/08/2005

TABLE 1: Bond Length (Å) of the PbS Monomer Obtained by Using Different Basis Sets on Pb[a]

lead basis set	bond length (Å)
experimental	2.287
(a) SBKJC	2.282
(b) SBKJC basis set + d (exponent = 0.149)	2.275
(c) SBKJC (completely decontracted)	2.271
(d) LANL2DZ	2.276
(e) LANL2DZ basis set + d (exponent = 0.164)	2.273
(f) LANL2DZ (completely decontracted)	2.272

[a] The basis set on sulfur is 6-31+G* for (a)−(f).

TABLE 2: NBO Analysis for PbS and CdS and $(PbS)_2$ and $(CdS)_2$[a,b]

				hybrids (%)		
orbital	occupancy			s	p	d
	(a) PbS and CdS					
PbS						
BD(S−Pb)	2.000	S	83.79	0.00	99.88	0.12
		Pb	16.21	0.00	99.17	0.83
BD(S−Pb)	2.000	S	83.79	0.00	99.88	0.12
		Pb	16.21	0.00	99.17	0.83
BD(S−Pb)	2.000	S	76.67	17.79	82.02	0.19
		Pb	23.33	8.77	91.13	0.10
LP(S)	2.000			83.05	16.94	0.00
LP(Pb)	1.999			92.77	7.23	0.00
CdS						
BD(S−Cd)	2.000	S	54.32	2.41	97.38	0.22
		Cd	45.68	98.98	0.04	0.98
LP(S)	1.997			98.23	1.75	0.02
LP(S)	1.958			0.00	99.95	0.05
LP(S)	1.958			0.00	99.95	0.05
	(b) $(PbS)_2$ and $(CdS)_2$					
$(PbS)_2$						
BD(Pb1−S2)	1.983	S	82.74	11.87	87.99	0.14
		Pb	17.26	3.24	96.36	0.40
BD(Pb1−S2)	1.876	S	93.68	0.15	99.76	0.09
		Pb	6.32	0.22	97.85	1.93
BD(Pb1−S4)	1.986	S	82.28	12.23	87.63	0.14
		Pb	17.72	3.55	96.07	0.37
BD(S2−Pb3)	1.986	S	82.28	12.23	87.63	0.14
		Pb	17.72	3.55	96.07	0.37
BD(Pb3−S4)	1.983	S	82.74	11.87	87.99	0.14
		Pb	17.26	3.24	96.36	0.40
BD(Pb3−S4)	1.876	S	93.68	0.15	99.76	0.09
		Pb	6.32	0.22	97.85	1.93
LP(S2)	1.990			76.00	23.98	0.02
LP(S4)	1.990			76.00	23.98	0.02
LP(Pb1)	1.996			93.29	6.71	0.00
LP(Pb3)	1.996			93.29	6.71	0.00
$(CdS)_2$						
BD(Cd1−S2)	1.991	S	81.00	4.43	95.44	0.13
		Cd	19.00	95.99	3.37	0.64
BD(S2−Cd3)	1.991	S	81.00	4.43	95.44	0.13
		Cd	19.00	95.99	3.37	0.64
LP(S2)	1.999			91.35	8.64	0.00
LP(S2)	1.967			0.00	99.94	0.06
LP(S4)	1.999			91.39	8.61	0.00
LP(S4)	1.967			0.00	99.94	0.06
LP(S4)	1.672			8.94	90.96	0.11
LP(S4)	1.660			0.00	99.86	0.14

[a] BD = two-center bond, LP =lone pair. [b] The connectivity is M1−S2−Pb3−S4−M1, where M = Pb or Cd

minimum was found. Energies were reevaluated using both the LANL2DZ+d (exponent = 0.164) basis set[28] and SBKJC+d (exponent = 0.149) basis set on lead. To test the accuracy of the SBKJC/6-31+G* basis set for obtaining geometries, clusters from the monomer to tetramer were also reoptimized with completely decontracted SBKJC and LANL2DZ basis sets on lead; however, the geometry differences were found to be negligible. Therefore the geometries of all clusters were optimized by using the SBKJC/6-31+G* basis set. CIS(D)[29] calculations were done with the B3LYP/SBKJC/6-31+G* geometries, using the LANL2DZ+d (Pb) and 6-31+G* (S) basis sets. Coordinates for all optimized geometries are given in the Supporting Information.

Results and Discussion

The Structures of the PbS Clusters. Table 1 defines the basis sets used in this work and lists the calculated bond lengths (Å) of the PbS monomer obtained with these basis sets. All calculated Pb−S bond lengths are in good agreement with the experimental value of 2.287 Å[30] in the monomer. The calculated vibrational frequencies of the PbS monomer varied from 422.9 to 446.7 cm^{-1}. When a typical scaling factor of 0.92 is applied, the calculated values fall in the range of 384−411 cm^{-1}, somewhat lower than the experimental value of 423.1 cm^{-1} (as measured in argon at 12 K[31]).

Figures 1 and 2 depict the geometries of the lowest energy structures of clusters from the monomer to the nonamer. The dimer (Figure 1) has C_{2v} symmetry, with a long Pb−Pb distance (3.460 Å). Comparing this value with the Ag−Ag distance (2.720 Å) of the AgBr dimer[32] and the Cd−Cd distance in the CdS dimer (2.833 Å),[21] it is clear that the Pb−Pb bond is significantly longer than the Ag−Ag bond, even if one considers the effect of atomic radii ($R_{Pb}/R_{Ag} \approx 1.03$, $R_{Cd}/R_{Ag} \approx 1.03$). Another interesting fact is that the bond angle of Pb−S−Pb (86.30°) is close to the typical bond angle characteristic of covalent sulfur bonds (92−99°). This suggests that the weak Pb−Pb interaction is accompanied by significant covalent Pb−S interactions. Indeed, as we will see below, covalent bonding is significantly more important in the PbS clusters than in the CdS clusters.

The trimer (Figure 1) is a folded structure with C_s symmetry and fold angles of 115.1° (Pb−S−Pb) and 99.56° (S−Pb−S). Again, the other bond angles centered on sulfur are in the range 85.8−92.8°, appropriate for covalent interactions. This structure can be basically described as consisting of two planes intersecting approximately at a right angle. This is completely different from the case of silver bromide and cadmium sulfide trimers (D_{3h}) shown below, which have a planar structure consisting of a triangular arrangement of metal atoms with anions bridging the metal−metal bonds.

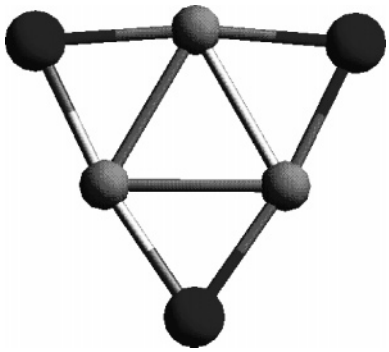

The tetramer (Figure 1) could be constructed from the trimer by adding one additional PbS unit to form a cube, and that is indeed what happens. All the edges of the cube (D_{2d}) are of equal length (2.67 Å), with their bond angles and dihedral angles close to 90°. Again, this structure is completely different than that found for AgBr and CdS (shown below) for which the metals form a tetrahedron and the anions cap the tetrahedral

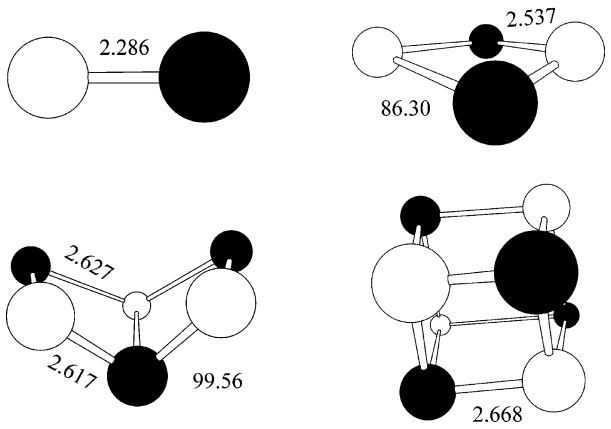

Figure 1. Optimized geometries of $(PbS)_n$ ($n = 1, 4$) with relevant geometrical parameters: solid atoms, lead; open atoms, sulfur.

faces. The PbS cubic structure is the basic unit of larger clusters, and it is also the primitive unit cell of galena.

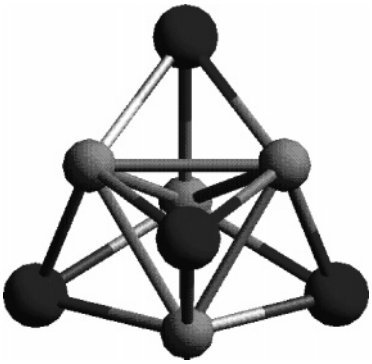

The pentamer (C_s) (Figure 2) could be described as an open structure obtained through insertion of an additional PbS unit into one plane of the cubic tetramer. In the hexamer (Figure 2), two cubes share a common face and a structure of D_{2h} symmetry is formed. The heptamer (Figure 2) is another open structure. The octamer (Figure 2) can be viewed as a cuboid obtained through stacking of three cubes (D_{2d}), but the Pb−S distance (3.047 Å) of the central cube is significantly longer than that of the other two cubes (2.738 Å). The nonamer (Figure 2) is formed from four cubes and has C_{2v} symmetry. Comparing this nonamer structure with the crystal structure of galena (Figure 2), we find that the nonamer is half of the rock-salt crystal's unit cell.

Importance of Covalent Interactions in the PbS Clusters. As mentioned earlier, the structures of the PbS clusters suggest that covalent bonding plays an important role in their formation. Here we compare the bonding in PbS and $(PbS)_2$ to that of CdS and $(CdS)_2$. We limit our discussion to these systems because they are the only clusters which are isostructural; however, we anticipate that our discussion will also be relevant to the larger clusters. The natural charges of Pb and S in the PbS monomer are 0.88/−0.88, respectively, while those of the CdS monomer are 1.00/−1.00. For the dimers, the corresponding charges are 1.04/−1.04 $(PbS)_2$ and 1.31/−1.31 $(CdS)_2$. In both cases, the natural charges indicate that the CdS bonds are more ionic than those of PbS. The natural bond orbitals, which are summarized in Table 2, provide a better picture of the bonding in these systems. For the monomer, PbS is described as a *triply* bound species (with very polar bonds, see Table 2), while Cd−S is

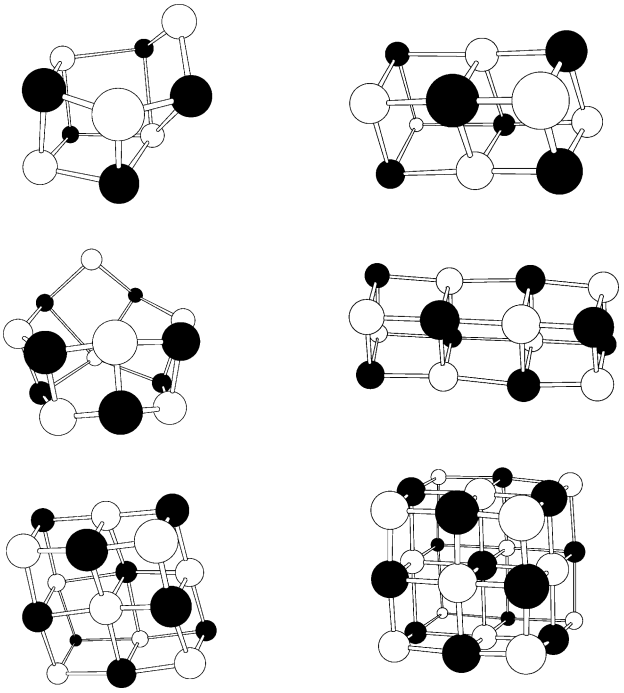

Figure 2. Optimized geometries of $(PbS)_n$ ($n = 5, 9$) and, for comparison, the PbS unit cell.

described as a *singly* bound species (the formal charges are in parentheses).

The dimers are described as resonance hybrids. $(PbS)_2$ exhibits cyclobutadiene-like structures.

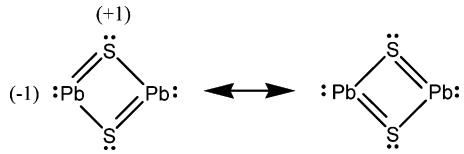

While $(CdS)_2$ is described by a much more ionic set of structures.

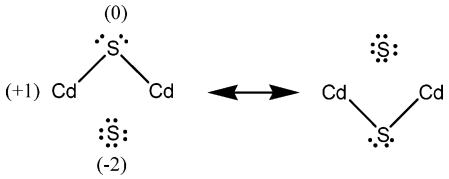

We conclude that covalent bonding plays an important role in the geometry preferences of PbS clusters, in contrast to our earlier work on AgBr and CdS, where metal−metal interaction dominates the geometrical preferences of these clusters.

Binding Energy and HOMO-LUMO Gaps of the PbS Clusters. The binding energies of all PbS neutral clusters calculated with different basis sets are given in Table 3. The binding energy per molecule, E_B/n, is defined for neutral clusters as:

$$E_B/n = -E_n/n + E_1 \text{ leading to } E_B = -E_n + nE_1$$

where E_n is the energy of neutral clusters with n PbS molecules, and E_1 is the energy of the monomer.

A plot of binding energy per molecule vs n obtained employing the SBKJC (a), SBKJC+d (b), and LANL2DZ+d (e) basis

TABLE 3: Binding Energies (kcal/mol) of PbS Clusters Calculated by Various Methods[a]

	basis set		
cluster	a	b	f
$(PbS)_2$	24.78	26.13	18.74
$(PbS)_3$	30.67	31.80	22.62
$(PbS)_4$	44.07	45.65	32.06
$(PbS)_5$	41.95	42.89	29.37
$(PbS)_6$	44.80	45.85	31.57
$(PbS)_7$	41.27	41.78	28.70
$(PbS)_8$	46.77	47.72	33.01
$(PbS)_9$	45.75	46.02	31.09

[a] The basis sets used (a, b, and f) are defined in Table 1.

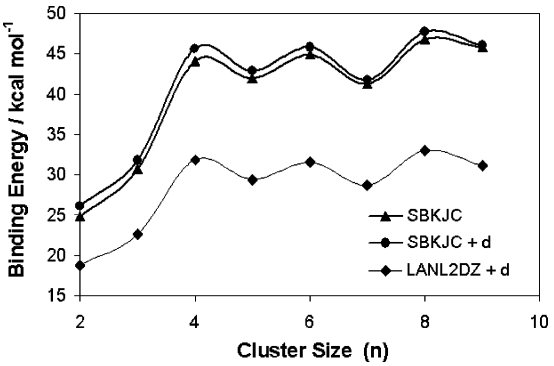

Figure 3. Binding energy as a function of cluster size.

TABLE 4: HOMO-LUMO Energy Gaps (eV) of PbS Clusters Calculated by Various Methods[a]

	basis set		
clusters	a	b	f
(PbS)	4.21	4.21	4.21
$(PbS)_2$	2.96	3.46	3.28
$(PbS)_3$	3.35	3.41	3.41
$(PbS)_4$	4.11	4.18	4.07
$(PbS)_5$	3.42	3.47	3.47
$(PbS)_6$	3.18	3.26	3.30
$(PbS)_7$	3.36	3.40	3.27
$(PbS)_8$	3.65	3.76	3.78
$(PbS)_9$	3.04	3.06	3.07

[a] The basis sets used (a, b, and f) are defined in Table 1.

sets on lead is shown in Figure 3. The binding energies increase monotonically from the monomer to the tetramer. From the pentamer to the nonamer, the binding energies of even number clusters are very similar to that of the tetramer, while the structures with odd numbers of PbS have lower binding energies. The lower binding energies of the pentamer and heptamer are expected because of their open structures, but the rather low binding energy for the nonamer is somewhat of a surprise. The LANL2DZ+d basis set yields consistently lower binding energies (~3 kcal/mol/PbS unit) than those derived from the SBKJC basis set, although the trends are identical.

Because of their relationship to the UV absorption spectra, the calculated HOMO-LUMO gaps of PbS clusters are tabulated in Table 4. The energy gaps derived from calculations with basis sets a, b, and e are plotted in Figure 4, along with the results obtained by explicitly calculating the wavelength of the transition with the largest oscillator strength at the CIS(D) level. The HOMO-LUMO gap oscillates from the monomer to the nonamer, suggesting alternating red shifts followed by blue shifts of the UV absorption band as the cluster grows. This behavior differs from that of silver bromide[32] and cadmium sulfide[21] quantum dots, for which an initial blue shift is followed by a monotonic red shift upon increasing cluster size.

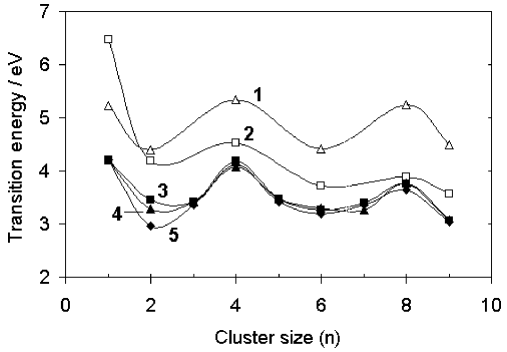

Figure 4. Excitation energy as a function of cluster size. (1) Experimentally found values (from ref 22). Calculated values: (2) CIS-(D). HOMO-LUMO gap: (3) SBKJC+d, (4) LANL2DZ, (5) SBKJC.

TABLE 5: CIS(D) Results for the Experimentally Observed PbS Clusters[a]

	transition		oscillator	excitation energy	
	orbital	state	strength f	eV	nm
PbS	$2\pi \rightarrow 5\sigma$	$^1\Sigma \rightarrow {}^1\Pi$	0.207	6.47	191.8
$(PbS)_2$	$3b_1 \rightarrow 4b_1$	$^1A_1 \rightarrow {}^1A_1$	0.052	4.18	296.8
$(PbS)_4$	$10t_2 \rightarrow 15t_2$	$^1A_1 \rightarrow {}^1A_1$	0.235	4.52	274.3
$(PbS)_6$	$3b_{1g} \rightarrow 6b_{2u}$	$^1A_g \rightarrow {}^1B_{3u}$	0.202	3.72	333.5
$(PbS)_8$	$8b_2 \rightarrow 9a_1$	$^1A_1 \rightarrow {}^1B_2$	0.315	3.88	319.9
$(PbS)_9$	$14a_1 \rightarrow 12b_2$	$^1A_1 \rightarrow {}^1B_2$	0.149	3.57	347.0

[a] The numbering systems start at the first valence orbital: 3s for S and 6s for Pb. The 4f and 5d orbitals on Pb are considered core orbitals and are not included.

The oscillating trend of the HOMO-LUMO gaps and CIS-(D) transition energies with increasing cluster size is in agreement with the experimental observation of the corresponding time-dependent UV absorption band of slowly growing PbS quantum dots (Figure 4). Ultra-small (<1 nm) uncapped PbS quantum dots, prepared through the electroporation of synthetic vesicles,[18] grow slowly on the exterior surface of the phospholipid bilayer, and exhibit the oscillating shift of their absorption band: 237.5 nm (monomer) → 282 nm (dimer) → 232 nm (tetramer) → 281 nm (hexamer) → 234.5 nm (octamer) → 278.5 nm (nonamer).[22] The CIS(D) calculations, summarized in Table 5, show a similar oscillating behavior. Only qualitative agreement is seen between the CIS(D) calculations and experiment; however, the CIS(D) results are significantly closer to experiment than the HOMO-LUMO gaps. There are three likely reasons for the lack of quantitative agreement. First, the experimental results refer to a situation in which the PbS clusters are actually absorbed on the surface of the phospholipid bilayer. Second, our basis sets are probably not of sufficient size to expect quantitative or near-quantitative accuracy. Finally, the geometries for both the ground and excited state are taken as the DFT optimized geometries of the ground states. Still, the CIS(D) approach, along with the HOMO-LUMO gaps, provide solid grounds on which to interpret the experimental results.

Summary

The structures of lead sulfide neutral clusters $(PbS)_{1-9}$ have been investigated by the use of density functional theory. In stark contrast to similar semiconductor clusters, even very small clusters ($(PbS)_n$, $n \geq 2$) begin to exhibit the character of the bulk galena crystal. The origin of this process is likely associated with the partial covalent nature of the Pb−S bond. With increasing cluster size, the HOMO-LUMO gap is found to exhibit an oscillating behavior, as are the CIS(D) transition energies. This trend is paralleled by the experimentally observed

oscillating red to blue shift of the UV absorption band of slowly growing PbS quantum dots in the molecular size regime.

Acknowledgment. This work was supported in part by grants from The Welch Foundation to D.S.M. (grant Y-0743) and to Z.A.S. (grant Y-0703).

Supporting Information Available: Tables of optimized geometries for PbS clusters. This material is available free of charge via the Internet at http://pubs.acs.org.

References and Notes

(1) Bliss, D. E.; Wilcoxon, J. P.; Newcomer, P.; Samara, G. A. *Mater. Res. Soc. Symp. Proc*. **1995**, *358*, 265−269.

(2) Gacoin, T. J.; Boilot, P.; Grandais, M.; Ricolloeau, C.; Chamarro, M. *Mater. Res. Soc. Symp. Proc*. **1995**, *358*, 247−252.

(3) Freedhoff, M. I.; Marchetti, A. P. In *Handbook of optical properties*; Hummel, R. E., Wissmann, P., Eds.; CRC Press: Boca Raton, FL, 1997; Vol. 2, pp 1−30.

(4) Tassoni, R.; Schrock, R. *Chem. Mater.* **1994**, *6*, 744−749.

(5) Sanctis, O. D.; Kadono, K.; Tanaka, H.; Sakaguchi, T. *Mater. Res. Soc. Symp. Proc.* **1995**, *358*, 253−258.

(6) Ward, A. J. I.; O'Sullivan, E. C.; Rang, J.; Nedeljkovic, J.; Patel, R. C. *J. Colloid Interface Sci.* **1993**, *161*, 316−320.

(7) Machol, J. L.; Wise, F. W.; Patel, R. C.; Tanner, D. B. *Phys. Rev. B* **1993**, *48*, 2819−2822.

(8) Moller, L.; Bein, T.; Herron, N. *Inorg. Chem.* **1989**, *28*, 2914−2919.

(9) Rossetti, R.; Hull, R.; Gilbson, J. M.; Brus, L. E. *J. Chem. Phys.* **1985**, *83*, 1406−1410.

(10) Weller, H. *Adv. Mater*. **1993**, *5*, 88−95.

(11) Brus, L. E. *J. Phys. Chem.* **1986**, *90*, 2555−2560.

(12) Wang, Y.; Suna, A.; Mahler, W.; Kasowski, R. *J. Chem. Phys*. **1987**, *87*, 7315−7322.

(13) Lippens, P. E.; Lannoo, M. *Phys. Rev. B* **1989**, *39*, 10935−10942.

(14) Kane, R. S.; Cohen, R. E.; Silbey, R. *J. Phys. Chem.* **1996**, *100*, 7928−7932.

(15) Tudury, G. E.; Marquezini, M. V.; Ferrira, L. G.; Barbosa, L. C.; Cesar, C. L. *Phys. Rev. B* **2000**, *62*, 7357−7364.

(16) Mian, M.; Harrison, N. M.; Saunders, V. R.; Flavell, W. R. *Chem. Phys. Lett*. **1996**, *257* (5, 6), 627−632.

(17) Hoffmann E.; Entel, P. *World Sci.* **1999**, *Nov. 2*, 1−8.

(18) Correa, N. M.; Zhang, H.; Schelly, Z. *J. Am. Chem. Soc*. **2000**, *122*, 6432−6434.

(19) Henglein, A.; Lilie, J. *J. Phys. Chem.* **1981**, *85*, 1246−1251.

(20) Gurin V. S. *Z. Phys. D* **1997**, *42*, 65−70.

(21) Zeng, H.; Marynick, D. S.; Schelly, Z. A. *Abstracts of Papers*; 225th National Meeting of the American Chemical Society, New Orleans, LA, March 23−27, 2003; American Chemical Society: Washington, DC, 2003; COLL-188. See also: Deglmann, P.; Ahlrichs, R.; Tsereteli, K. *J. Chem. Phys.* **2000**, *116*, 15851597. Troparevsky, M. C.; Chelikowsky, J. R. *J. Chem. Phys.* **2001**, *11*, 943−949. Joswig, J.; Springborg, M.; Seifert, G. *J. Phys. Chem. B* **2000**, *104*, 2617−2622. Maroulis, G.; Pouchan, C. *J. Phys. Chem. B* **2003**, *107*, 10683−10686.

(22) Wu, S.; Zeng, H.; Schelly, Z. A. *Langmuir* **2005**, *21*, 686−691.

(23) Frisch, M. J.; Trucks, G. W.; Schlegel, H. B.; Scuseria, G. E.; Robb, M. A.; Cheeseman, J. R.; Zakrzewski, V. G.; Montgomey, J. A.; Stratmann, R. E., Jr.; Burant, J. C.; Dapprich, S.; Millam, J. M.; Daniels, A. D.; Kudin, K. N.; Strain, M. C.; Farkas, O.; Tomasi, J.; Barone, V.; Cossi, M.; Cammi, R.; Mennucci, B.; Pomelli, C.; Adamo, C.; Clifford, S.; Ochterski, J.; Petersson, G. A.; Ayala, P. Y.; Cui, Q.; Morokuma, K.; Malick, D. K.; Rabuck, A. D.; Raghavachari, K.; Foresman, J. B.; Cioslowski, J.; Ortiz, J. V.; Baboul, A. G.; Stefanov, B. B.; Liu, G.; Liashenk, A.; Piskorz, P.; Komaromi, I.; Gomperts, R.; Martin, R. L.; Fox, D. J.; Kieth, T.; Al-Laham, M. A.; Peng, C. Y.; Wong, M. W.; Pople, J. A. *GAUSSIAN98*, Revision A.9; Gaussian Inc.: Pittsburgh, PA, 1998.

(24) Frisch, M. J.; Trucks, G. W.; Schlegel, H. B.; Scuseria, G. E.; Robb, M. A.; Cheeseman, J. R.; Montgomery, J. A., Jr.; Vreven, T.; Kudin, K. N.; Burant, J. C.; Millam, J. M.; Iyengar, S. S.; Tomasi, J.; Barone, V.; Mennucci, B.; Cossi, M.; Scalmani, G.; Rega, N.; Petersson, G. A.; Nakatsuji, H.; Hada, M.; Ehara, M.; Toyota, K.; Fukuda, R.; Hasegawa, J.; Ishida, M.; Nakajima, T.; Honda, Y.; Kitao, O.; Nakai, H.; Klene, M.; Li, X.; Knox, J. E.; Hratchian, H. P.; Cross, J. B.; Bakken, V.; Adamo, C.; Jaramillo, J.; Gomperts, R.; Stratmann, R. E.; Yazyev, O.; Austin, A. J.; Cammi, R.; Pomelli, C.; Ochterski, J. W.; Ayala, P. Y.; Morokuma, K.; Voth, G. A.; Salvador, P.; Dannenberg, J. J.; Zakrzewski, V. G.; Dapprich, S.; Daniels, A. D.; Strain, M. C.; Farkas, O.; Malick, D. K.; Rabuck, A. D.; Raghavachari, K.; Foresman, J. B.; Ortiz, J. V.; Cui, Q.; Baboul, A. G.; Clifford, S.; Cioslowski, J.; Stefanov, B. B.; Liu, G.; Liashenko, A.; Piskorz, P.; Komaromi, I.; Martin, R. L.; Fox, D. J.; Keith, T.; Al-Laham, M. A.; Peng, C. Y.; Nanayakkara, A.; Challacombe, M.; Gill, P. M. W.; Johnson, B.; Chen, W.; Wong, M. W.; Gonzalez, C.; Pople, J. A. *Gaussian 03*, Revision C.02; Gaussian, Inc.: Wallingford, CT, 2004.

(25) Becke, A. D. *J. Chem. Phys*. **1993**, *98*, 5648.

(26) Lee, C.; Yang, W.; Parr, R. G. *Phys. Rev. B* **1988**, 785.

(27) Haroold, B.; Stevens, W. J.; Krauss, M. *Chem. Phys. Lett*. **1984**, *109*, 212−16.

(28) Wadt, W. R.; Hay, P. J. *J. Chem. Phys*. **1985**, *82* (1), 284−298.

(29) Head-Gordon, M.; Rico, R. J.; Oumi, M.; Lee, T. J. *Chem. Phys. Lett*. **1994**, *219*, 21−29.

(30) Teichman, R. A., III; Nixon, E. R. *J. Mol. Spectrosc.* **1975**, *54*, 78−86.

(31) Marino, C. P.; Guerin, J. D.; Nixon, E. R. *J. Mol. Spectrosc.* **1974**, *51*, 160−165.

(32) Zhang, H.; Schelly, Z. A.; Marynick, D. S. *J. Phys. Chem.* **2000**, *104*, 6287−6294.